Available online at www.sciencedirect.com
ScienceDirect
Journal of Power Sources 178 (2008) 59–63
JOURNAL OF POWER SOURCES
www.elsevier.com/locate/jpowsour

Short communication

Highly efficient and durable anode-supported SOFC stack with internal manifold structure

M. Yokoo *, Y. Tabata, Y. Yoshida, K. Hayashi, Y. Nozaki, K. Nozawa, H. Arai

NTT Energy and Environment Systems Laboratories, NTT Corporation, 3-1, Morinosato-Wakamiya, Atsugi-shi, Kanagawa 243-0198, Japan

Received 28 September 2007; received in revised form 12 December 2007; accepted 12 December 2007
Available online 23 December 2007

Abstract

We have developed a solid oxide fuel cell (SOFC) stack with an internal manifold structure. The stack, which is composed of 25 anode-supported 100-mm-diameter SOFCs, provided an electrical conversion efficiency of 56% (based on the lower heating value of methane, which was used as a fuel) and an output of 350 W when the fuel utilization, current density, and operating temperature were 75%, 0.3 A cm^{-2}, and 1073 K, respectively. The electrical efficiency and the output were maintained for 1100 h. The cell voltage fluctuation was ±2% for 25 cells. The relationship between average cell voltage and current density in the 25-cell stack was as almost the same as that in the 1- and 10-cell stacks, which suggests that our stack provides almost the same cell performance regardless the number of the cells.

Keywords: Solid oxide fuel cell; Cell stack; High electrical conversion efficiency; Durability

1. Introduction

A solid oxide fuel cell (SOFC) system, which provides the highest electrical conversion efficiency of various kinds of fuel cell systems, is a promising next generation power source [1–3]. We have been developing an SOFC system for use in our communication bases, where electricity is more important than heat as an energy source. The fuel cell itself and the cell stack that employs it are key technologies for establishing a high-performance fuel cell system. Therefore, we have been focusing on their development.

Of the various kinds of SOFC structure, the anode-supported planar type SOFC is a promising candidate. We have already developed an SOFC that provides a very high-power density [4,5]. Several original technologies were used in developing the cell. To reduce the electrical resistance of the cell, scandia and alumina stabilized zirconia (SASZ), which has a high ionic conductivity, was employed as the electrolyte material and the anode substrate [4,5]. In addition, the electrolyte thickness was reduced by using an anode-supported structure formed by co-firing the electrolyte and the anode substrate [4,5]. $LaNi(Fe)O_3$ (LNF) [6–9] was used as the cathode material. LNF has high electronic conductivity [6,9], good catalytic activity [6,9], and resistance to Cr poisoning [7,8]. Furthermore, the characteristics of a stack that uses our anode-supported cell accommodated in metallic separators (interconnects) were reported in our previous work [10]. The stack had an external manifold structure. One- and three-cell stacks with 60-mm-diameter cells exhibited a dc electrical conversion efficiency of 53% (based on the lower heating value (LHV) of fuel) and a durability of 1000 h.

In this paper, it is shown that a new type of stack with an internal manifold structure provides a high electrical efficiency of 56% (based on the LHV of fuel) and a long operating time that exceeds 1000 h.

2. Stack design

The stack was constructed by combining a lot of power generation units, each of which was mainly composed of an anode-supported type cell and five metal plates (cathode interconnector, cathode plate, cell holder, anode plate, and anode interconnector) as shown in Fig. 1. The geometry of the anode-supported type cell is summarized in Table 1. The kind of the metal was a corrosion resistive ferritic stainless steel. The force across the stack is evenly applied to the cell holding part and the manifold parts. The stack has one fuel feeding manifold, one air

* Corresponding author. Tel.: +81 46 240 2572; fax: +81 46 270 2702.
E-mail address: m.yokoo@aecl.ntt.co.jp (M. Yokoo).

0378-7753/$ – see front matter © 2007 Elsevier B.V. All rights reserved.
doi:10.1016/j.jpowsour.2007.12.044

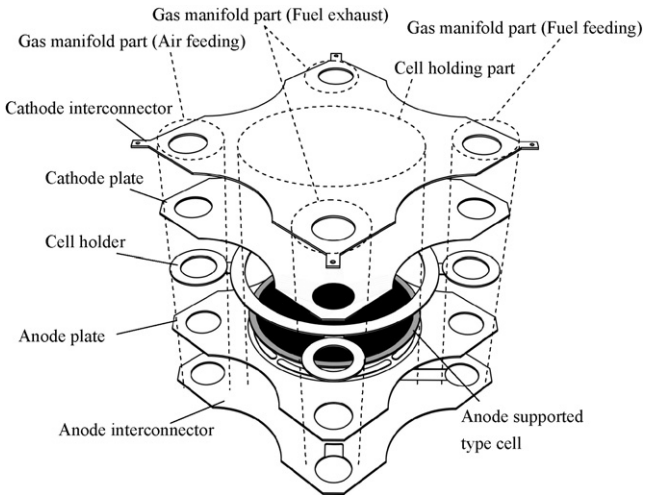

Fig. 1. Structure of power generation unit.

feeding manifold, and two fuel exhaust manifolds. That is the stack has two fuel exhaust paths, which results in efficient fuel evacuation. By using thin metal spacers, the top and the bottom of the power generation unit are kept almost parallel. This allows us to increase easily the number of power generation units in a cell stack. Porous metal, which is easily compressed, was placed between the anode and the anode plate. The porous metal is then compressed, the shape of the metal changes along the curvature of the anode, and the metal fills the space between the anode and the anode plate, thus achieving good electrical contact between them. The cathode was coated with ceramic paste to enhance the current collection performance [11]. The gas manifold and flow path were designed by using the thermo-fluid simulator, FLUENT [12]. Though the diameter of the gas manifold should be minimize to make stack compact, it should be maximize to achieve the uniform gas distribution. In addition, the height of the flow path should be large for a low pressure loss, but it should be small for the uniform gas distribution. The diameter of the gas manifold and the height of the flow path were set at 20 and 0.55 mm, respectively, so that the fluctuation in the flow rates of fuel and air for each cell was less than 1%. The stack design is summarized in Table 2.

3. Experiment

The performance of 1-, 10-, and 25-cell stacks was investigated. A force of about 60 kgf was applied to the stacks by using metal bellows as shown in Fig. 2. There are 25 power generation units in the stack shown in Fig. 2 and the stack size was about 140 mm × 140 mm × 140 mm.

The configuration of the evaluation system is shown in Fig. 3. Methane with a purity of 99.5% (CH_4: 99.5%, N_2: 0.05%, CO_2: 0.45%) was used as the fuel after the anode had been reduced by hydrogen, and dry air was used as the oxidant. The methane was reformed in the steam reformer and the reformed gas was fed to the SOFC stack. The steam needed for the steam reforming was generated in a vaporizer. The flow rate of water was determined so that the steam to carbon ratio was 3.0. The composition of the reformed gas, which was analyzed by gas chromatography (GC), is shown in Table 3. Here, the methane was below the GC detection limit. The SOFC stack and steam reformer were installed in different electric furnaces both of which had three zones. The

Table 1
Geometry of anode-supported type cell

Diameter (mm)	
Anode	100
Electrolyte	100
Cathode	88
Thickness (mm)	
Anode	1.1
Electrolyte	0.02
Cathode	0.06
Active electrode area (cm^2)	60

Table 2
Summary of stack design

Feature	Effect
Two fuel exhaust paths	Efficient fuel evacuation
Parallel arrangement of both top and bottom of power generation units	Easy stacking of power generation units
Porous metal placed between anode and anode plate	Enhanced electrical contact
Cathode coated with ceramic paste	Enhanced electrical contact
Flow path designed by thermo-fluid simulator	Almost equal distribution of fuel and air

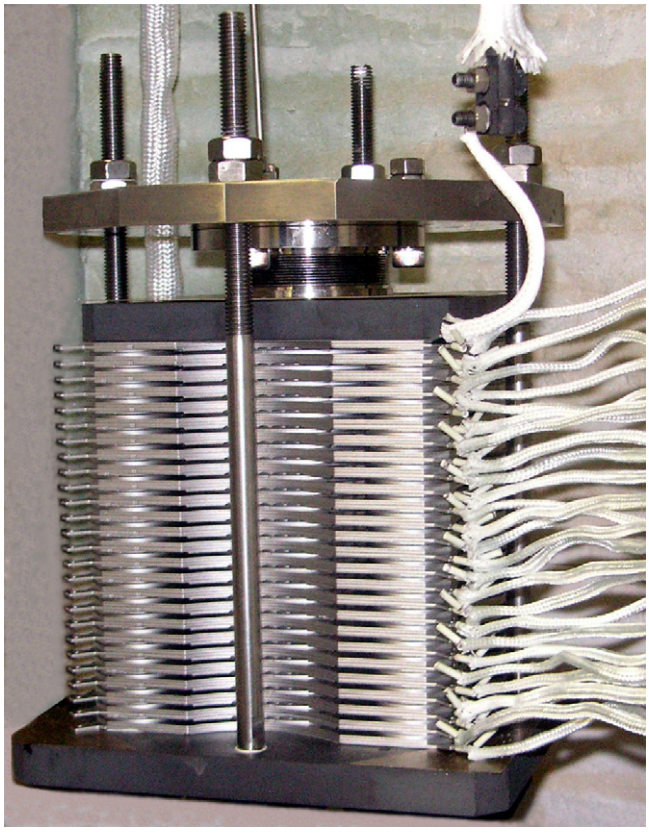

Fig. 2. Twenty-five-cell stack.

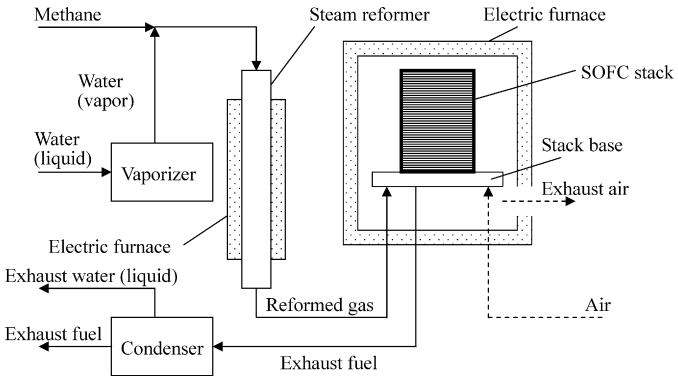

Fig. 3. Configuration of evaluation system.

Table 3
Composition of reformed gas

Gas	Composition (%)
H_2	55
H_2O	28
CO	12
CO_2	5

Table 4
Furnace temperatures (K)

Electric furnace for SOFC stack	
Top	1073
Middle	1073
Bottom	1073
Electric furnace for steam reformer	
Inlet	923
Middle	1073
Outlet	973

setting temperatures are listed in Table 4. The amount of current was controlled by using external electronic load equipment. The exhaust fuel from the stack was fed to a condenser to separate water. The exhaust air from the stack was discharged into the atmosphere via the joint gap of the electric furnace.

When the cell voltage and power density were measured as a function of current density, the gas feeding condition was set as shown in Table 5. The respective fuel and oxygen utilizations were 60% and 15% in all the stacks when the current was 18 A (current density: 0.3 A cm^{-2}). When the effect of fuel utilization on stack performance was investigated, the flow rate of fuel was varied while the current density and flow rate of air were kept constant.

Table 5
Gas feeding condition for cell voltage and power density measurement as function of current density

	Flow rate of methane (ml min^{-1})	Flow rate of air (l min^{-1})
1-Cell stack	53	2
10-Cell stack	525	20
25-Cell stack	1313	50

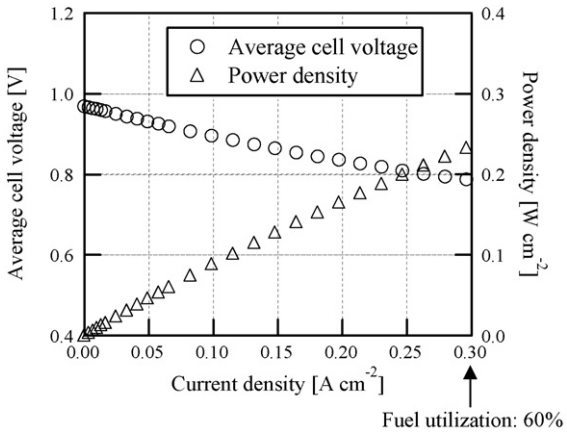

Fig. 4. Average cell voltage and power density as a function of current density in 25-cell stack.

4. Results and discussion

Average cell voltage and power density as a function of current density in 25-cell stack are shown in Fig. 4. A stack output of 355 W was achieved when the current density was 0.3 A cm^{-2} (fuel utilization: 60%). The effect of fuel utilization was investigated in a 25-cell stack by changing the fuel flow rate. The current density was kept at 0.3 A cm^{-2} and the oxygen utilization was kept at 15%. The stack output decreased with the fuel utilization as shown in Fig. 5. This is because the stack voltage decreased with the fuel utilization since the molar fraction of the steam increased with fuel utilization. By contrast, the electrical efficiency at gross dc, which was calculated by using the LHV of methane, increased with fuel utilization as shown in Fig. 5. Although the stack voltage decreased with increasing fuel utilization, the decrement in the amount of unused fuel led to a higher energy conversion ratio. The stack output and electrical efficiency were 350 W and 55.8%, respectively, when the fuel utilization was 75%.

The temporal change in the electrical efficiency in a 25-cell stack is shown in Fig. 6. The current density, fuel utilization, and oxygen utilization were kept at 0.3 A cm^{-2}, 75%, and 15%, respectively. An electrical efficiency of greater than 55.5% was maintained for over 1100 h. Although the electrical efficiency

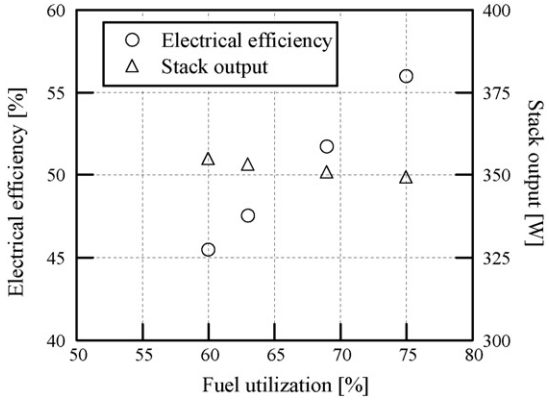

Fig. 5. Relationship between electrical efficiency at gross dc (LHV) and fuel utilization in 25-cell stack.

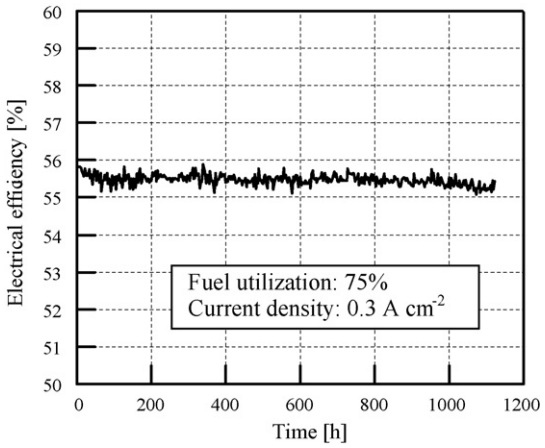

Fig. 6. Temporal change in electrical efficiency at gross dc (LHV) in 25-cell stack.

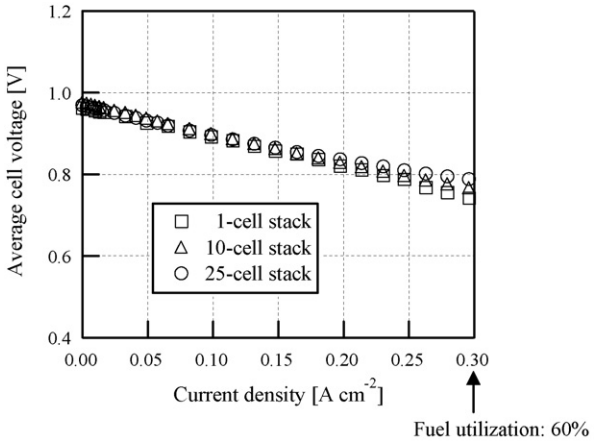

Fig. 7. Relationship between average cell voltage and current density in 1-, 10-, and 25-cell stack.

decreased by 0.3% in first 100 h, the degradation in the electrical efficiency was nearly 0 for the last 1000 h. The summary of 25-cell stack performance is shown in Table 6. This stack performance is reasonable since over 6000 h of operation has been achieved in a 1-cell stack experiment [10]. The resistance of the cathode to Cr poisoning [7,8] is one of the reasons for this good stability. The reason for the degradation during the first 100 h can be considered as follows. The stack is not as tall when functioning at its designed operating temperature as it was when constructed at room temperature. It is estimated that the stack height stabilizes after the first 100 h of operation, and then the stack performance also stabilizes. A discussion of this phenomenon will be important future work and the deformation of the stack after the power generation test will be investigated. In addition, there was oxide scale on the surface of the separator after the power generation test. It is also important to investigate the state of the oxide scale. Furthermore, the degradation of less than 0.1% was observed between 1000 and 1100 h. A long-term test with longer operating time can clarify the stability.

The relationships between average cell voltage and current density in 1-, 10-, and 25-cell stacks are shown in Fig. 7. These relationships were almost the same regardless of the number of the cells in the stack, which suggests that our stack provides almost the same cell performance regardless the number of the cells. However, the relationships between the average cell voltage and current density differed slightly. When the current density is larger than 0.2 A cm^{-2}, the average cell voltage in 10-cell stack was slightly higher than that in the 1-cell stack and the average cell voltage in the 25-cell stack was slightly higher than that in the 10-cell stack. It is estimated that this is because the stack temperature, which was not measured in the experiments, increased slightly with the number of cells in the stacks. The individual cell voltages in the stacks at a current density of 0.3 A cm^{-2} are shown in Fig. 8. The cells were numbered form the bottom. There was very little fluctuation in the cell voltages in each stack. The deviance of the cell voltage δ, which was defined as follows:

$$\delta = \max_{1 \le i \le N} \frac{|V_i - \bar{V}|}{\bar{V}} \times 100 \quad (1)$$

was less than 1% for a 10-cell stack and less than 2% for a 25-cell stack. Here, V_i is the cell voltage, N is the number of power generation units in the stack, and $\bar{V}$ is the average cell voltage. From this result, it can be estimated that fuel and air were distributed almost equally in each cell. Furthermore, it can be said that a good electrical connection was achieved between the metallic separators and the cell for all the cells in the stacks regardless of their number. This is mainly because the all the separators in the stacks were kept parallel and any cell warpage was absorbed by the porous metal placed between the anode and the anode separator.

The degradation in the cell voltage after 1100 h of operation in a 25-cell stack is shown in Fig. 9. In this figure, the plus and minus values indicate decrements and increments in the cell voltages, respectively. Although the cells placed at the top and

Table 6
Summary of the 25-cell stack performance

Stack output (W)	350
Efficiency (%)	55.5
Stable operating time (h)	1100

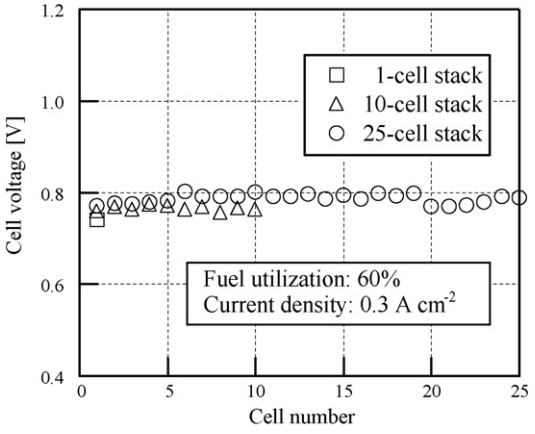

Fig. 8. Fluctuation in cell voltages at a current density of 0.3 A cm^{-2} in 1-, 10-, and 25-cell stacks.

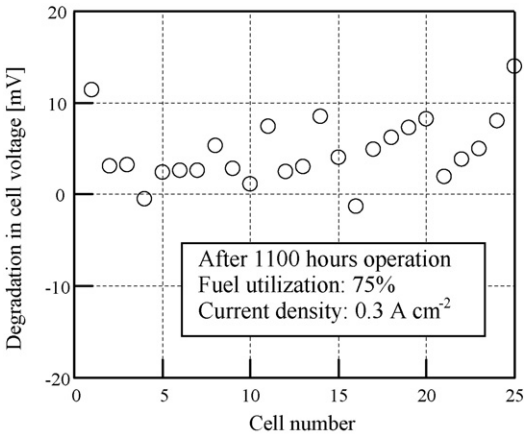

Fig. 9. Degradation in cell voltage for 1100 h operation in 25-cell stack.

bottom exhibit slightly more degradation, there was no significant tendency for the other cells relating to cell position. This result confirms the equal distribution of fuel and air. The greater degradation in the edge cells was considered to be because the temperatures of the edge cells were slightly lower than those of the other cells. It is considered that the lower temperature led to a poorer electrical connection and this, in turn, caused the greater degradation. The reason will be investigated in future work.

5. Conclusion

We have developed an SOFC stack with an internal manifold structure. The gas flow path was designed by using numerical simulation technology so that the fuel and air are distributed to each SOFC almost equally. By using thin metal spacers, the top and the bottom of the power generation unit are kept almost parallel. This makes it easy to increase the number of power generation units in a cell stack. Methane was used as the fuel and it was reformed in a steam reformer, which was separate from the SOFC stack. The stack, which was composed of 25 anode-supported 100-mm-diameter SOFCs, provides an electrical efficiency of 56% (based on the LHV of methane) and an output of 350 W when the fuel utilization, current density, and operation temperature were 75%, 0.3 A cm^{-2}, and 1073 K, respectively. The electrical efficiency and the output were maintained for 1100 h. The fluctuation in the cell voltages was ±2% among 25 cells. The relationship between average cell voltage and the current density in the 25-cell stack was almost the same as those in the 1- and 10-cell stacks, which suggests that our stack provides almost the same cell performance regardless the number of the cells.

In future, the SOFC stack with a larger output will be developed by increasing the cell size and the number of the cell in the stack.

References

[1] T. Ujiie, ECS Transactions 7 (2007) 3–9.
[2] A. Wayne, Surdoval, ECS Transactions 7 (2007) 11–15.
[3] Bert Rietveld, ECS Transactions 7 (2007) 17–23.
[4] H. Orui, K. Watanabe, R. Chiba, M. Arakawa, Journal of Electrochemical Society 151 (2004) A1412–A1427.
[5] H. Orui, K. Nozawa, R. Chiba, T. Komatsu, K. Watanabe, S. Sugita, H. Arai, M. Arakawa, ECS Transactions 7 (2007) 225–261.
[6] R. Chiba, F. Yoshimura, Y. Sakurai, Solid State Ionics 124 (1999) 281–288.
[7] T. Komatsu, H. Arai, R. Chiba, K. Nozawa, M. Arakawa, K. Sato, Electrochemical and Solid State Letters 9 (2006) A9–A12.
[8] T. Komatsu, H. Arai, R. Chiba, K. Nozawa, M. Arakawa, K. Sato, Journal of Electrochemical Society 154 (2007) B379–B382.
[9] R. Chiba, H. Orui, T. Komatsu, Y. Tabata, K. Nozawa, H. Arai, M. Arakawa, K. Sato, ECS Transactions 7 (2007) 1191–1200.
[10] S. Sugita, H. Arai, Y. Yoshida, H. Orui, M. Arakawa, ECS Transactions 5 (2007) 491–497.
[11] Y. Yoshida, S. Sugita, H. Arai, M. Arakawa, The 15th Symposium on Solid Oxide Fuel Cells in Japan Extended Abstracts, 2006, pp. 200–203 (in Japanese).
[12] T.M. Prinkey, A.W. Rogers, S.R. Gemmen, American Society of Mechanical Engineering Heat Transfer Division 369-4 (2001) 291–300.